Mon. Not. R. astr. Soc. (1982) **201**, 991–1008

Very extended ionized gas in radio galaxies – I. A radio, optical and ultraviolet study of PKS 2158 – 380

R. A. E. Fosbury *Royal Greenwich Observatory, Herstmonceux Castle, Hailsham, East Sussex BN27 1RP*

A. Boksenberg* and M. A. J. Snijders *Department of Physics and Astronomy, University College London, Gower Street, London WC1E 6BT*

I. J. Danziger *European Southern Observatory, Karl-Schwarzschild Strasse-2, Garching bei Munchen, Germany D-8046*

M. J. Disney *Department of Applied Mathematics and Astronomy, University College, Cardiff CF1 1XL*

W. M. Goss *Kapteyn Laboratory, University of Groningen, Postbus 800, Groningen, The Netherlands*

M. V. Penston *Astronomy Division ESTEC, ESA, Villafranca Satellite Tracking Station, Apartado 54065, Madrid, Spain and Royal Greenwich Observatory, Herstmonceux Castle, Hailsham, East Sussex BN27 1RP*

W. Wamsteker *European Southern Observatory, Casilla 16317, Santiago 9, Chile and Astronomy Division ESTEC, ESA, Villafranca Satellite Tracking Station, Apartado 54065, Madrid, Spain*

K. J. Wellington *CSIRO Division of Radiophysics, PO Box 76, Epping, NSW 2121, Australia*

A. S. Wilson *Astronomy Program, University of Maryland, College Park, MD 20742, USA*

Received 1982 April 7; in original form 1982 January 25

Summary. Several radio galaxies are known which exhibit extended emission-line regions covering tens of kiloparsecs. The gas which extends to a radius of 15 kpc in PKS 2158 – 380 is in a high state of ionization and has a spectrum which is inconsistent with local photoionization by hot stars. *IUE* observations show a point source of ultraviolet radiation at the nucleus which can be fitted by a power law with a spectral index of -1.4. If the gas is distributed within the galaxy in such a way as to cover a large fraction of the sky at large distances from the nucleus, this ultraviolet source is sufficiently luminous to photoionize the whole emission-line region. We suggest that this sky coverage can be obtained if the gas is in the form of a severely warped disc which may have resulted from the capture and disruption by the

* Present address: Royal Greenwich Observatory.

elliptical of a small gas-rich galaxy. The velocity field of the gas is studied using high-dispersion, long-slit spectroscopy of the [O III] lines. By fitting to power-law photoionization models, we estimate the total mass of gas responsible for the extended emission to be $\sim 10^8 M_\odot$. The radio structure is double but with an unusually asymmetric flux ratio which may be related to the location of the galaxy towards the edge of a small group. The capture of gas by an elliptical galaxy and the subsequent dissipative evolution may be responsible for the nuclear activity and associated phenomena we observe in some radio galaxies.

1 Introduction

Classical extragalactic double radio sources seem always to be associated with elliptical galaxies. On close examination, however, many of these radio ellipticals exhibit evidence of abnormal quantities of dust and gas. This has led to the rather general idea that the origin of the radio galaxy phenomenon and the associated nuclear activity may be related in some way to the source and evolution of the interstellar component.

The particular relationship between dust lanes and radio sources in ellipticals has been investigated by Kotanyi & Ekers (1979) who show that there is a tendency for the plane of the dust lane to be perpendicular to the axis defined by the double radio source. In some cases, the projected rotation axis of the gaseous component has been measured spectroscopically (Simkin 1979; Graham 1979; Goss *et al.* 1980; Danziger, Goss & Wellington 1981; Caldwell & Phillips 1981) and this has shown a weak tendency to be aligned with the radio axis. Jenkins & Scheuer (1980) and Jenkins (1981) have, however, suggested that no alignment exists between the radio axes and *stellar* rotation axes of a sample of eight galaxies. These structures of dust and gas do not appear to be similar to the massive discs of spiral galaxies and may prove to be transient features occupying only a small fraction of the total lifetime of an elliptical. In the case of the radio galaxy Centaurus A (NGC 5128, Graham 1979), it has been suggested by Tubbs (1980) that the disc is the result of recent accretion and is presently relaxing into a plane of symmetry of the elliptical by undergoing differential precession in a prolate gravitational potential.

From a programme of long-slit spectroscopy of Parkes radio galaxies, a number of objects which show a strong emission-line spectrum from a region of large spatial extent have been found. The emission-line surface brightness is not particularly strongly concentrated towards the nucleus, in marked contrast to the few spiral Seyfert galaxies known to show any extended emission (e.g. NGC 3516, Ulrich & Péquignot 1980). The most extreme examples of the phenomenon are the galaxies associated with PKS 2158 – 380 (Bolton & Shimmins 1973), PKS 0349 – 27 (Bolton, Clarke & Ekers 1965; Searle & Bolton 1968; Christiansen *et al.* 1977) and PKS 2048 – 57 (Mills, Slee & Hill 1961). The extended emission associated with PKS 2048 – 57 (≡ IC 5063) has already been discussed by Caldwell & Phillips (1981) and by Danziger, Goss & Wellington (1981) while PKS 0349 – 27, which shows strong [O III] and [O II] lines extending over 50 kpc ($H = 50\,\mathrm{km\,s^{-1}\,Mpc^{-1}}$) from the nucleus, is the subject of a later paper in this series. Other examples are 3C 120, where the outlying emission has been studied in detail by Baldwin *et al.* (1980), and Mk 335 (Heckman & Balick 1981).

There are two reasons why we consider a detailed study of this phenomenon in an archetypal object to be important. First, there is the question of the origin and evolution of the gaseous content of elliptical galaxies and its relationship to the origin of the radio galaxy phenomenon. Secondly, and perhaps of more general relevance to the formation and structure of ellipticals, there is the opportunity the extended emission affords us to study the velocity field and consequently the mass distribution out to radii unreachable by absorption-line techniques.

In such a study, ultraviolet observations are particularly relevant to establishing the ionization mechanism. Measurements reaching as close as is feasible to the Lyman continuum wavelength can currently be made with *IUE* and provide the best direct indication of the ionizing flux beyond 912 Å. In the past, for example, they have confirmed the presence of photoionizing sources in Seyfert galaxies (e.g. Boksenberg *et al.* 1978; Clavell *et al.* 1980; Bergeron, Maccacaro & Perola 1981) and their absence in NGC 1052 (Fosbury *et al.* 1981).

In this paper we present the results of such an observational study of PKS 2158 – 380 made using a variety of radio, optical and ultraviolet techniques. The discussion addresses the problems of the ionization mechanism and the physical and dynamical states of the gas and its evolution. We find that the interpretation of the ionization mechanism imposes constraints on the geometrical configuration of the gas which are consistent with its recent origin and may imply that the evolution is rapid.

2 Observations

Our original interest in PKS 2158 – 380 was excited by low-resolution, long-slit optical spectroscopy which showed a high-ionization emission-line spectrum from a region about half an arcmin (30 kpc) in extent. Here we present further optical spectrophotometry, high-resolution spectroscopy and ultraviolet spectrophotometry designed to study both the ionization structure and the velocity field. In addition we have obtained new photographic plates, optical and infrared broad-band photometry and continuum radio maps. These observations are described below.

2.1 OPTICAL AND ULTRAVIOLET SPECTROPHOTOMETRY

Table 1 is a journal of the spectrophotometric observations made with the Image Dissector Scanner (IDS) on the Anglo-Australian telescope (AAT), the University College London Image Photon Counting System (IPCS) on the ESO 3.6-m telescope and with the long- and short-wavelength cameras at the low-resolution of the *International Ultraviolet Explorer* satellite (*IUE*). The various aperture sizes are listed; for the optical observations, the longer sides of the aperture were oriented east–west and, for the respective *IUE* observations, these were at position angles given in Table 1.

The IPCS observation was made using an extended data memory (Boksenberg 1978) which allowed a two-dimensional format of 1500 wavelength elements by 70 spatial

Table 1. Spectrophotometric observations.

Date (UT)	Instrument	Wavelength range (Å)	Resolution (FWHM) (Å)	Aperture (arcsec)	PA of long axis (deg)	Exposure (min)
1975 Aug 5	AAT IDS	3600–6200	12	3×6	90	48
1975 Aug 6	AAT IDS	4800–7300	12	3×6	90	48
1976 Aug 2	AAT IDS	3600–7000	10	2×4	90	32
1978 Aug 30	ESO IPCS	3500–7100	12	4×116	90	40
1978 Dec 19	*IUE* SWP	1150–1950	6	10×20	159	120
1979 May 28	*IUE* LWR	1900–3200	8	10×20	150	417
1979 June 1	*IUE* SWP	1150–1950	6	10×20	149	120
1979 Nov 24	*IUE* SWP	1150–1950	6	10×20	146	406

increments of 1.65 arcsec on the sky. All of the optical observations were reduced to a scale of flux per unit wavelength using observations of white dwarfs (Oke 1974) as standard stars. Due to the superior photometric conditions at the time of observation, the IPCS data are used in preference for absolute photometry although the IDS observations have been used to supplement the relative line intensity measurements near the nucleus where the IPCS count rate in the strong lines was close to the saturation limit. Some selected IPCS data are illustrated in Fig. 1 which relate to a summed region around the nucleus and another at a mean radius of 8 kpc. A grey-scale representation of the whole two-dimensional frame has already been published (Fosbury 1980).

The *IUE* data were first reduced using the standard IUESIPS package. The spectra were then re-extracted from the geometrically- and photometrically-corrected images using the software package developed at University College London (Snijders 1980), correcting an early error in the camera intensity transfer function (Holm 1979). The emission-line-free continuum given in Table 2 is the average of the calibrated data over bins of order 100 Å wide. The best of the three short-wavelength exposures (SWP 7215) is illustrated in Fig. 2.

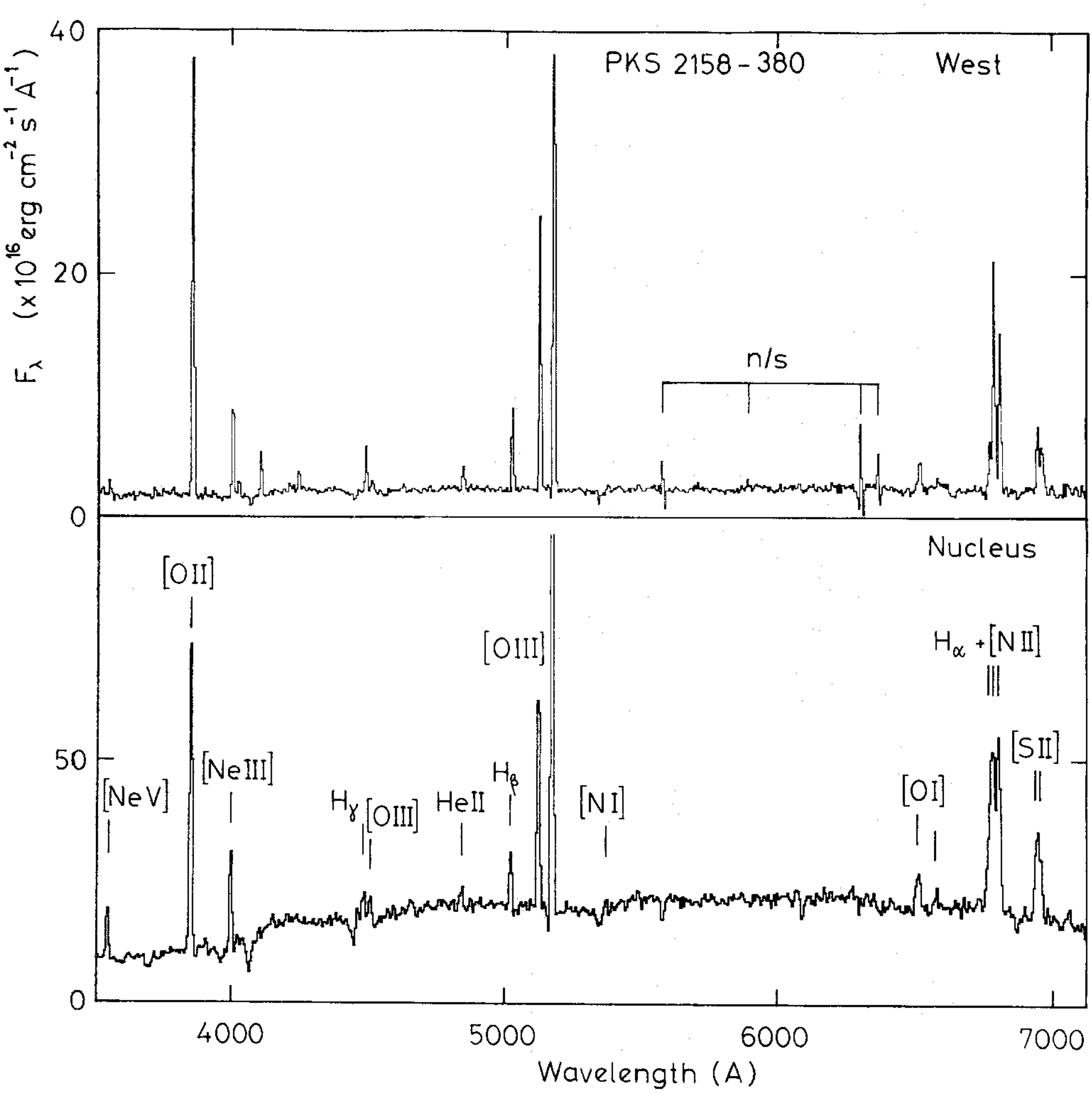

Figure 1. Low-dispersion optical spectra of the nucleus and the extended emission. The data are integrated over apertures of 5×4 arcsec^2 and 6.6×4 arcsec^2 respectively with the long axis EW. For the extended emission, the aperture is centred 7.4 arcsec to the west of the nucleus.

Table 2. Line-free continuum fluxes.

Central wavelength (Å)	Observed flux ($\times 10^{16}$ erg cm^{-2} s^{-1} $Å^{-1}$)	Error*	Instrument
7000	32.21		IPCS
6700	33.88		
6600	34.67		
6400	33.88		
6300	37.41		
6200	36.56		
6100	35.08		
6000	35.48		
5900	35.40		
5800	34.28		
5700	34.20		
5600	33.96		
5500	34.67		
5400	31.62		
5300	29.79		
4900	32.06		
4800	32.81		
4700	30.90		
4600	29.11		
4400	26.06		
4300	26.42		
4200	26.98		
4100	20.75		
3700	14.62		
3600	14.76		
3050	6.8	1.6	*IUE* LWR
2950	7.9	1.4	
2850	6.6	1.1	
2750	6.0	0.8	
2650	6.0	1.3	
2550	8.6	1.8	
2450	10.2	2.7	
2350	5.4	3.5	
2250	7.3	3.5	
2150	7.9	4.4	
2050	5.3	3.3	
1925	10.3	1.4	*IUE* SWP
1875	8.2	1.2	
1825	8.4	1.7	
1775	9.4	2.1	
1728	5.9	2.1	
1670	6.1	2.6	
1630	$\leqslant 8.2$	(3σ limit)	
1570	8.7	3.1	
1525	6.7	2.3	
1476	10.4	3.0	
1420	10.6	1.7	
1375	10.5	2.8	
1325	5.8	1.8	
1281	8.7	1.8	
1232	12.7	2.2	

*The errors quoted for the *IUE* measurements are 1σ deviations computed when binning the data plus a 10 per cent calibration uncertainty. The optical measurements are subject to a calibration uncertainty of about 20 per cent.

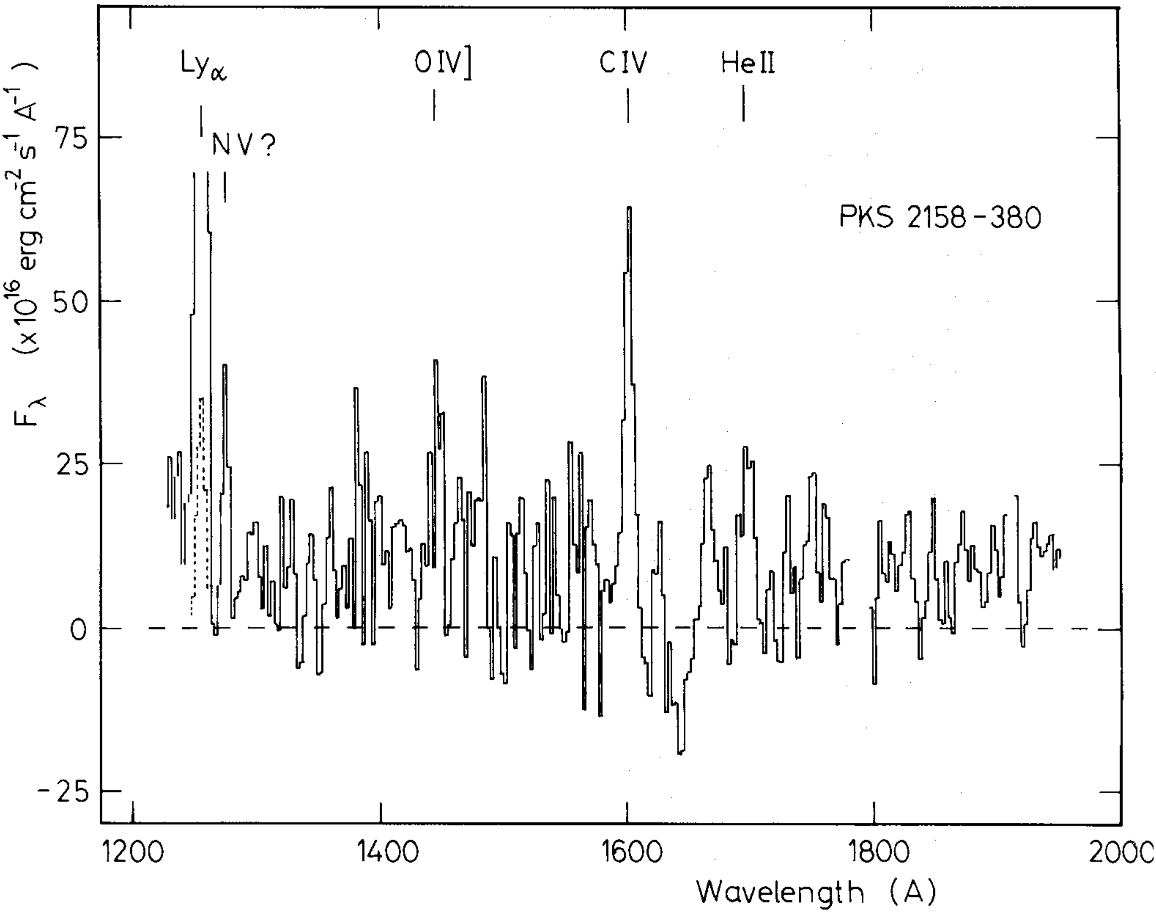

Figure 2. The short-wavelength *IUE* spectrum. The He II and Ly α lines are spatially extended within the large aperture. The dashed Ly α is reduced in scale by a factor of 10.

Two additional characteristics of the *IUE* spectra should be noted at this point. The He II λ 1640 and Lyman α emission lines are spatially extended while the short-wavelength continuum is indistinguishable from a point-source.

2.2 OPTICAL AND INFRARED PHOTOMETRY

UBV photometry of the galaxy and its bright spiral companion (Galaxy D, Plate 2) was obtained with the ESO 1-m telescope during 1978 September. The *J*, *H* and *K* magnitudes of the nucleus have been measured by Alan Moorwood using the ESO 3.6-m telescope. All of these data appear in Table 3. The errors, in *V*, $B-V$ and $U-B$ are estimated to be 0.02, 0.05 and 0.05 mag respectively, while those in *J*, *H* and *K* are about 0.06 mag.

2.3 OPTICAL HIGH-DISPERSION SPECTROSCOPY

To obtain information on the velocity field of the ionized gas, we observed the [O III] λλ 4959, 5007 lines with the IPCS at the 82-cm focal length camera of the RGO spectrograph on the AAT. The dispersion was 10 Å mm^{-1} and the slit width corresponded to 0.7 arcsec. The velocity and spatial resolutions (FWHM) were respectively 30 km s^{-1} and 2.7 arcsec. We used a two-dimensional format of 500 wavelength elements by 38 spatial increments covering a total slit length of 33 arcsec. Six 1000-s integrations were made with the slit

Table 3. Optical and infrared photometry.

Aperture diameter (arcsec)	Band λ_{eff} (μm) *U* 0.36	*B* 0.44	*V* 0.55	*J* 1.20	*H* 1.64	*K* 2.19
PKS 2158 – 380						
88	–	14.85	13.91	–	–	–
62	15.19	14.90	14.03	–	–	–
44	15.23	15.01	14.14	–	–	–
32	15.36	15.23	14.29	–	–	–
22	15.61	15.39	14.47	–	–	–
7*	–	–	–	13.20	12.50	12.14
Spiral companion						
62	15.81	15.72	15.11	–	–	–

* The beam was peaked at the centre with a FWHM of 7 arcsec.

passing through the nucleus at position angles 0, 30, 60, 90, 120 and 150 degrees. These observations are illustrated in Plate 1. The spectra were wavelength-calibrated with reference to a copper/argon discharge lamp exposed before and after each observation. The mean heliocentric redshift of the [O III] lines is $z = 0.03333 \pm 0.00003$ corresponding to a distance of 200 Mpc ($H = 50\,\mathrm{km\,s^{-1}\,Mpc^{-1}}$ is used throughout this paper).

2.4 RADIO OBSERVATIONS

When this investigation was started, the radio structure of PKS 2158 – 380 was unknown. Consequently we made continuum maps at frequencies of 1.4 and 5 GHz respectively with the Fleurs Synthesis telescope (FST) near Sydney and the Very Large Array (VLA) in New Mexico. The 1.4-GHz observation, cleaned to a circular beam with HPBW 50 arcsec, is shown in Fig. 3. We have measured the optical position of the galaxy to be at α (1950) $21^h\,58^m\,17^s.21 \pm 0.02$, δ (1950) $-38°\,00'\,50''.8 \pm 0''.2$ and this is marked on the radio map. The VLA observation was made as part of a survey of Parkes radio galaxies (Ekers *et al.* in preparation). A map with a resolution of 34 × 10 arcsec is shown superimposed on the high-contrast print in Plate 2(a). The VLA reveals no point source coincident with the nucleus of the galaxy having a flux density at 5 GHz greater than 7 mJy. Flux density measurements between frequencies of 80 MHz and 14.8 GHz appear in Table 4. With the exception of the

Table 4. Radio flux density measurements. These are taken from Ekers *et al.* (in preparation) which gives the original references.

Frequency (MHz)	Flux density (Jy)
80	25
160	7.1
408	4.12
1 420	1.53
2 700	1.01
5 000	0.59
14 800	0.332

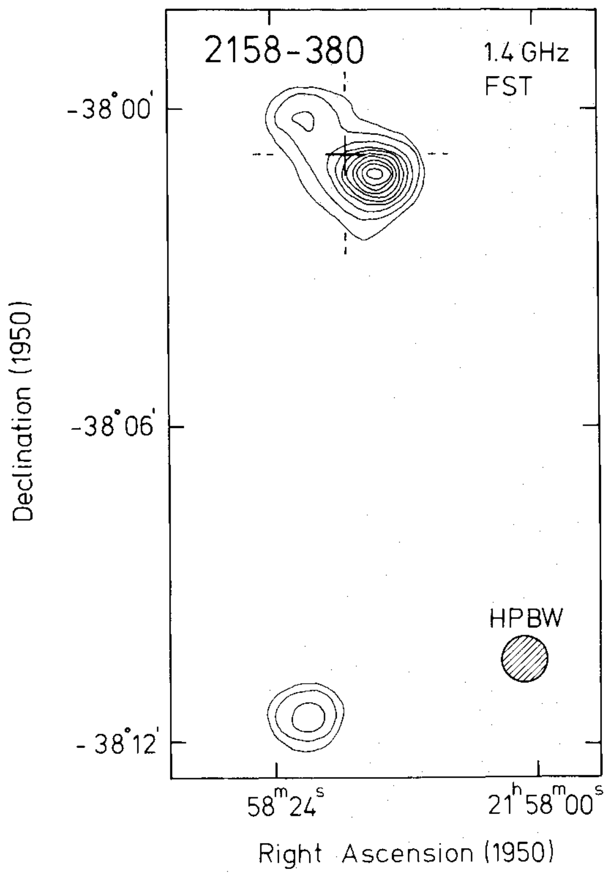

Figure 3. The 1.4-GHz continuum map made with the Fleurs Synthesis telescope. The contour levels are at 50, 100, 200, 300, 400, 500, 600, 700, 800 and 900 mJy/beam area. The optical position of the galaxy is marked with a cross. The southern source is unresolved and presumably unrelated.

observation at 80 MHz, the data are well fitted by a power law with spectral index $\alpha = -0.72$ ($f_\nu \propto \nu^{+\alpha}$). The monochromatic power at 1.4 GHz is 6.0×10^{23} WHz^{-1} sr^{-1}.

2.5 OPTICAL IMAGING

On the ESO/SRC sky survey, the galaxy associated with PKS 2158 − 380 appears as the dominant elliptical in a small group of about 10 members. The face-on spiral 4 arcmin to the south-west is undisturbed. On the IIIa-J film, the elliptical shows some evidence of extended structure, reaching over 2 arcmin to the south-east. We have obtained higher resolution, prime focus plates with both the ESO 3.6-m and the Anglo-Australian telescopes. Two prints from the AAT plate (No. 1886, 80 min IIIa-J + GG 385) are shown in Plates 2 and 3. The B and R ESO plates (No. 865, 20 min IIa-O + GG 385; No. 1051, 45 min IIa-F + RG 630) confirm the S-shaped structure shown around the nucleus in Fig. 5. The absence of this structure on the near-infrared exposure (No. 1780, 45 min 4N + RG 715) suggests, however, that it consists of line emission and not stellar continuum radiation. This, as we shall see, is consistent with the spectroscopy.

The radial velocities of three other galaxies in the group have been measured using the IPCS on the ESO 3.6-m telescope. For the galaxies marked B, C and D in Plate 2 the redshifts are respectively 0.0324, 0.0338 and 0.0335 ± 0.0003.

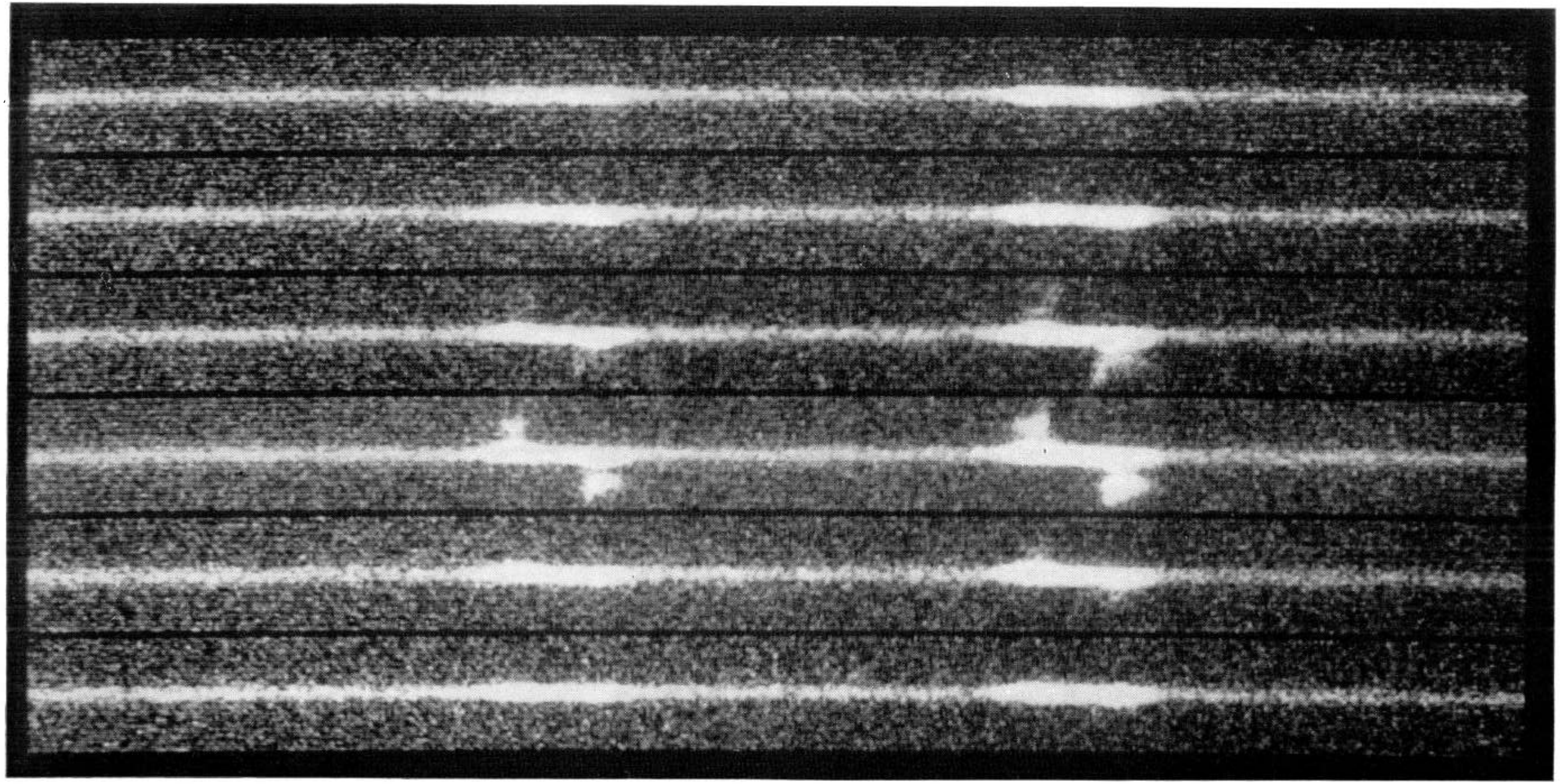

Plate 1. Grey scale representations of the high-dispersion spectra of the [O III] $\lambda\lambda4959$, 5007 region. From top to bottom the slit position angles are 0, 30, 60, 90, 120 and 150 degrees.

[facing page 998]

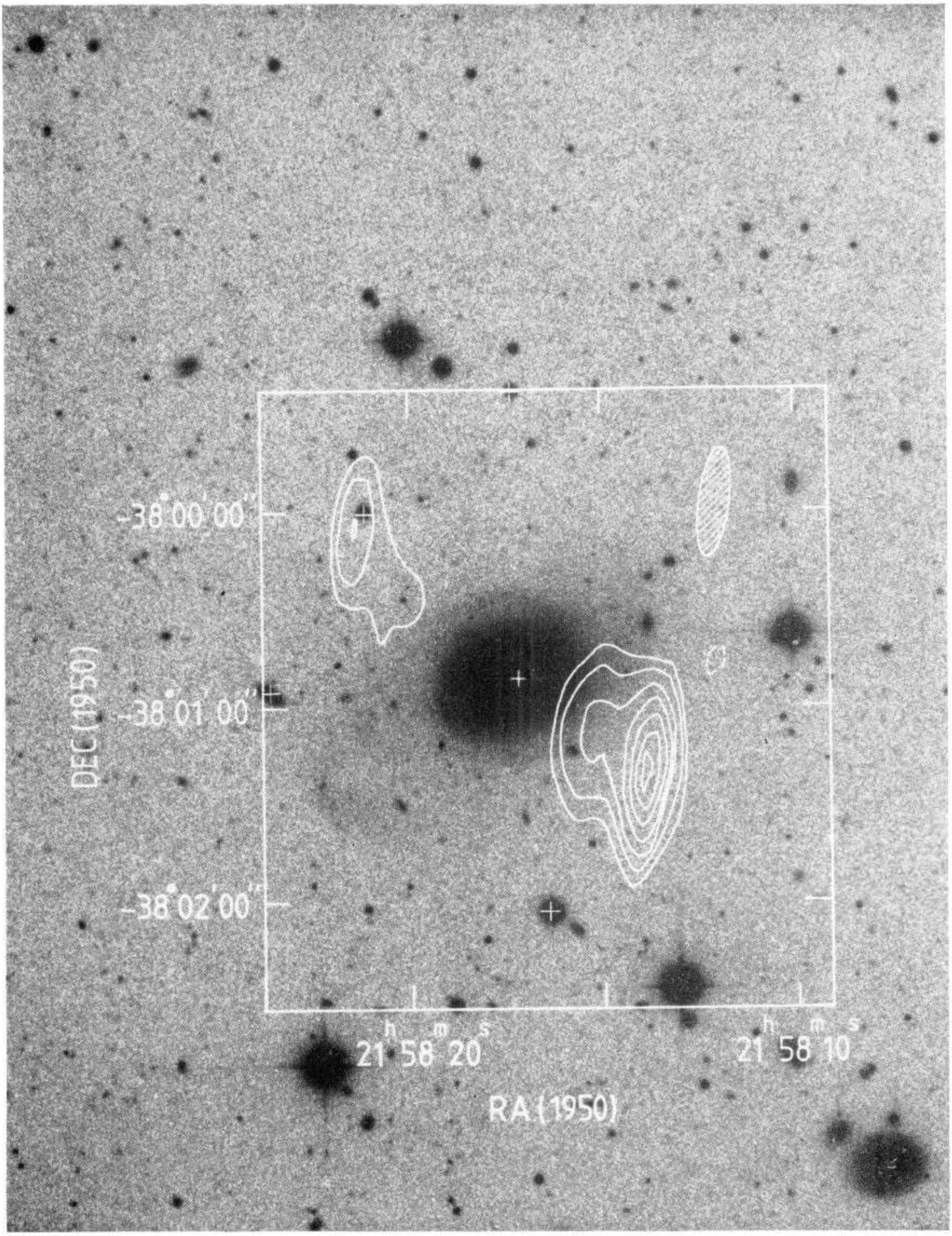

Plate 2. (a). A high-contrast derivative of the IIIa-J AAT plate overlaid with the 5-GHz VLA map. The peak radio flux is 222 mJy and the contours are at 5, 10, 20, 30, 50, 70 and 90 per cent.

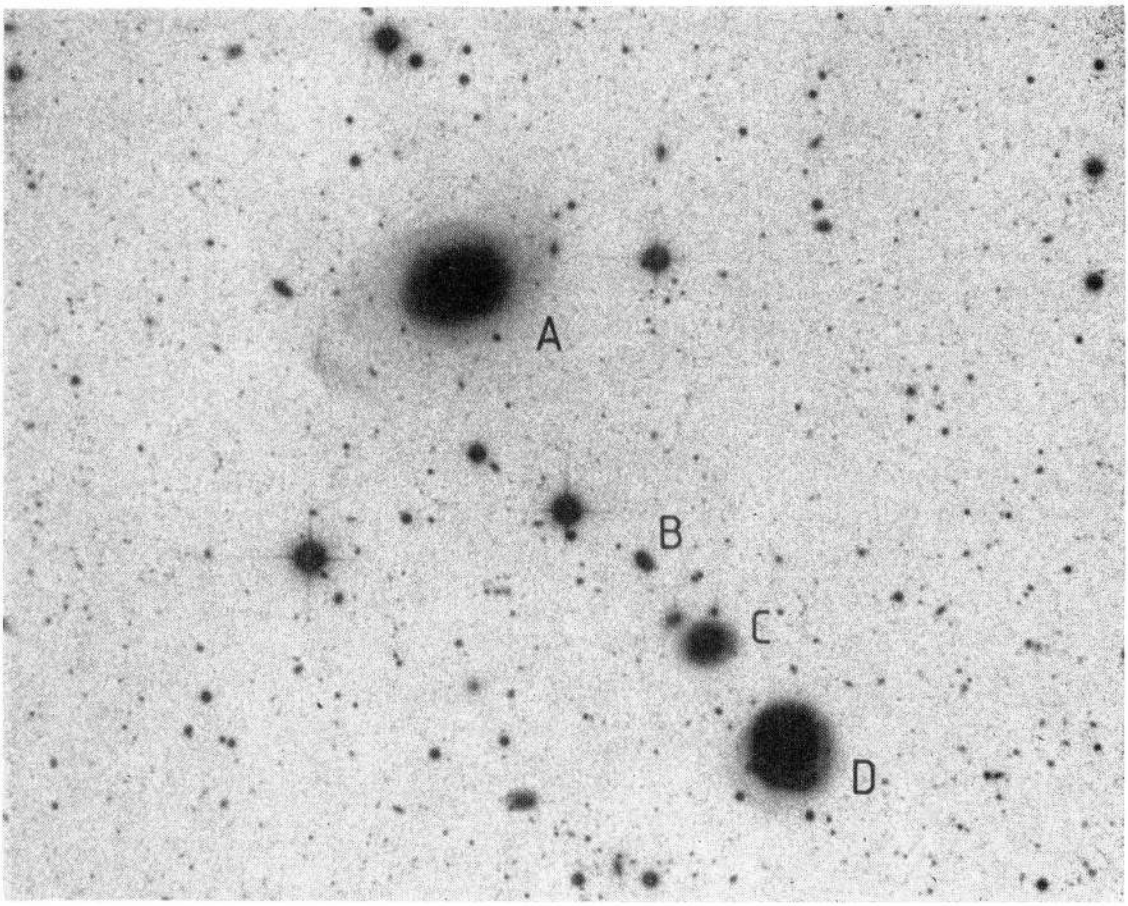

Plate 2 (b). Identification of the galaxies discussed in the text.

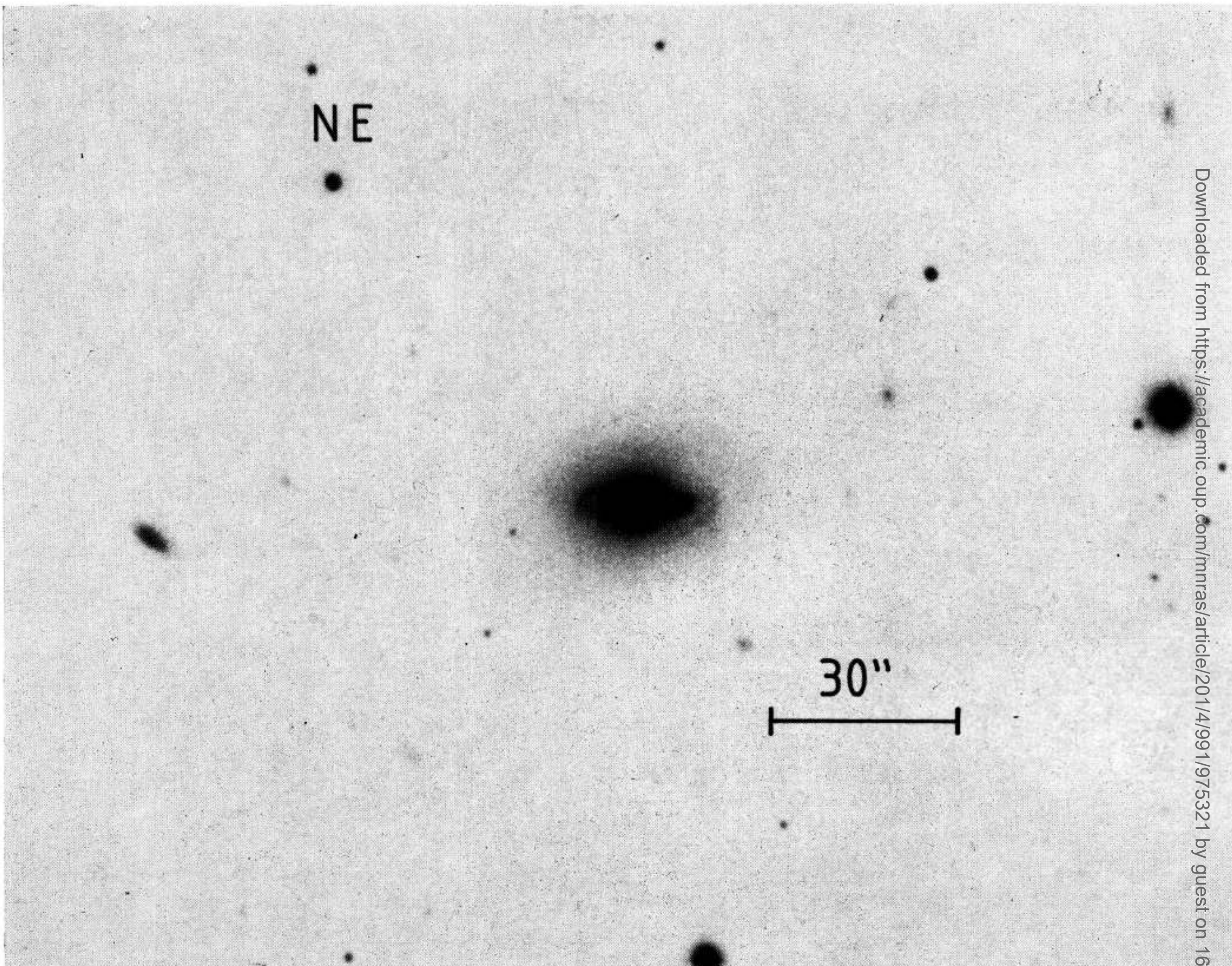

Plate 3. An unsharp masked print from the same AAT plate showing the S-shape structure which we believe to be predominantly due to line emission.

3 Results

The results of these observations are discussed in two parts. First, the physical conditions within the emission-line region and the source of ionization are established from the optical and ultraviolet spectrophotometry. Secondly, the high-dispersion spectroscopy is used to examine the geometric and kinematic state of the ionized gas. As far as is possible, the motions of the stars in the elliptical component are investigated using the low-dispersion data.

3.1 THE IONIZED GAS

We measured the optical emission-line fluxes from both the IDS and IPCS spectrophotometry. The data were corrected for extinction in our Galaxy corresponding to $E(B-V) = 0.08$ mag appropriate to this region of sky (de Vaucouleurs, de Vaucouleurs & Corwin 1976). Four columns of line intensities are listed in Table 5. In the first two, the relative intensities are given from the nuclear region, measured from both the IPCS and the IDS data. The [O III] intensity is missing from the IPCS column because of instrumental saturation. When comparing the two sets of figures it should be noted that the IPCS and IDS observing apertures were not precisely the same shape. We estimate the error (1σ) in

Table 5. Relative emission-line strengths corrected for a reddening of $E_{B-V} = 0.08$.

		Nucleus		Extended	*IUE*
		(IPCS)	(IDS)	emission	aperture
		5 × 4	6 × 3	2 × (5 × 4)	
				R = 8 kpc	
1216	Lyα				2070
1405	O IV (+ Si IV)				142
1548	C IV				299
1640	He II				220
1666	O III]				<102
2800	Mg II				<53
3425	[Ne V]	78	–	<11	66
3727	[O II]	429	404	609	492
3869 +3968	[Ne III]	164	136	159	185
4340	Hγ	49	44	49	54
4363	[O III]	40	30	13	31
4686	He II	28	25	22	29
4861	Hβ	100	100	100	100
4959 +5007	[O III]	–	1870	1250	–
5199	[N I]	15	12	<5	15
5876	He I	25	10	<5	17
6300 +6363	[O I]	96	77	73	109
6563	Hα	303	340	270	355
6548 +6584	[N II]	404	453	263	356
6725	[S II]	211	185	168	234
F(Hβ) (erg cm^{-2} s^{-1})		2.0×10^{-14}		0.9×10^{-14}	3.0×10^{-14}
L(Hβ) (erg s^{-1})		1.3×10^{41}		0.6×10^{41}	2.0×10^{41}

Note: < represents a 3σ upper limit.

the tabulated line intensities relative to Hβ to be given approximately by $\pm(n+10$ per cent), where $n=2$ for the optical observations and 40 for the ultraviolet. The absolute photometry could be subject to a systematic error of 20 per cent. The third column gives the intensities from the outer parts of the galaxy. The data were summed in three spatial increments from each side of the galaxy with inner and outer edges corresponding to projected radii of 5.8 and 10.7 kpc. Finally, in order to make comparisons with the ultraviolet emission lines, the IPCS data were summed along a slit length of 12 arcsec, corresponding approximately to the east–west dimension of the *IUE* aperture in the mean position angle of the two short-wavelength observations. The optical and ultraviolet apertures are still not the same shape, but the high-dispersion spectroscopy confirms that the emission is much less extended in the north–south direction, so the effect of this should be small. Also given in the table are the fluxes and luminosities corrected to the rest frame at $z=0.033$. The ultraviolet line fluxes given in Table 5 represent the emission summed over the entire *IUE* aperture; no attempt has been made to separate it into nuclear and extended components.

The continuum energy distribution from the UV to the IR is illustrated in Fig. 4. The longer wavelengths are dominated by late-type stars, but below 3000 Å a flatter-spectrum component is evident. Although this behaviour could be due to a spatially compact population of hotter stars, these would not provide sufficient ionization to explain the emission lines. We therefore exmaine the assumption that the UV continuum is emitted by a nuclear non-thermal source. The best-fitting power law below 2800 Å is

$$L_\nu = 0.30\times10^{28}\,(\nu/\nu_0)^{-1.4}\ \mathrm{erg\,s^{-1}\,Hz^{-1}}$$

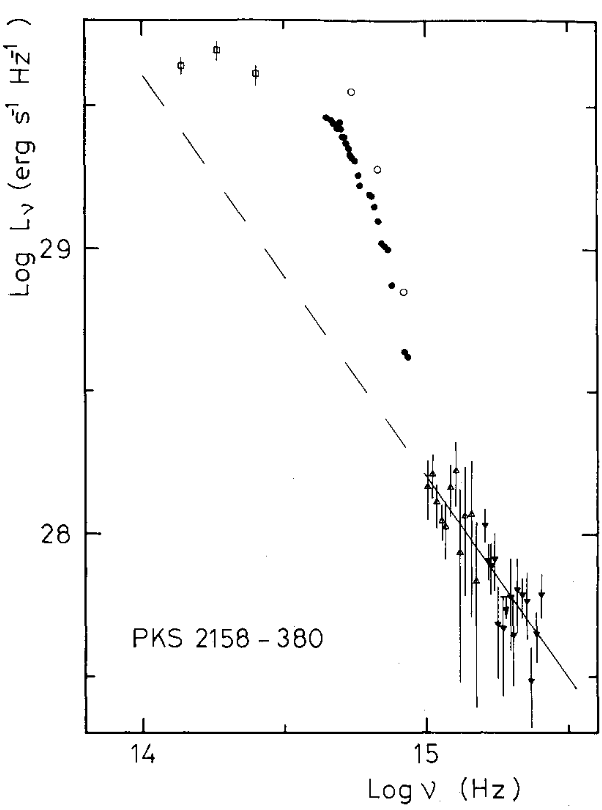

Figure 4. The infrared to ultraviolet energy distribution. The observed fluxes have been converted to luminosities assuming a distance of 200 Mpc and a galactic reddening corresponding to $E_{B-V}=0.08$. □ *JHK* photometry, 7 arcsec HPBW. ○ *UBV* photometry, 22 arcsec aperture. ● Optical spectrophotometry, long slit × 4 arcsec. ▲, ▼ *IUE* LWR and SWP spectrophotometry, large aperture. The straight line is a power-law fit to the *IUE* data shortward of 2800 Å. The optical spectrophotometry is subject to a calibration uncertainty of about 20 per cent; the other errors are discussed in the text.

where ν_0 is the frequency of the Lyman limit. If this extended into the infrared with an index steeper than −1.4, it would have been detected by our *JHK* photometry although the ultraviolet measurements would certainly allow an index as flat as −1. The observed He II λ4686/Hβ ratio also suggests $\alpha \simeq -1.4$ (Penston & Fosbury 1978) near the nucleus although Table 5 does show that the degree of ionization is slightly lower in the outer region. If extrapolated to shorter wavelengths, the best fit corresponds to an integrated Lyman continuum luminosity of 2.5×10^{43} erg s^{-1}, which is to be compared with the total emission-line luminosity of $\geqslant 1.1 \times 10^{43}$ erg s^{-1}. This quantitative similarity, together with the high-ionization state of the extended emission, suggests that the whole emission-line region may be photoionized by the nuclear source of UV radiation. Under this assumption, recombination theory gives an expression for f, the fraction of sky seen from the nucleus which is covered by optically thick gas:

$$f \sim 0.4 L_{41}(\mathrm{H}\beta)(-\alpha)/L_{28},$$

here L_{41} (Hβ) and L_{28} are respectively the total Hβ luminosity in units of 10^{41} erg s^{-1} and the continuum luminosity at the Lyman limit in units of 10^{28} erg s^{-1} Hz^{-1}. With a spectral index of −1.4 and the observed luminosities, $f \sim 1$, which can be taken as an important constraint on the geometrical distribution of the ionized gas. For example, a thin, planar disc would imply $f \ll 1$ and would therefore be inconsistent with the data. It is clear that our measurement of the UV continuum luminosity and hence this conclusion of large sky coverage depends on the actual value of the reddening, not only on our line-of-sight to the nucleus but also throughout the radio galaxy. However, several factors reassure us that this is likely to be small. For the continuum itself, there is the absence of a significant λ2200 dust signature, although the application of the galactic reddening curve to internal extinction in a radio galaxy is highly uncertain. There is also the aforementioned consistency between the observed UV spectral index and the He II λ4686/Hβ ratio. For the emission-line region, the first column of Table 5 offers several useful line ratios. From Hα/Hβ, Hβ/Hγ, Lyα/Hβ and He II λλ1640/4686, using the appropriate low-density recombination values given by Osterbrock (1974), Krolik & McKee (1978) and Seaton (1978) and the galactic extinction law given by Seaton (1979), we derived a weighted mean $E(B-V) = 0.08 \pm 0.04$ appropriate to the region bounded by the *IUE* aperture. Since this reddening is of such low significance, we have made no attempt to make any further correction to the line or continuum intensities. The Balmer decrement in the outlying emission (last column of Table 5) is very close to its case B value.

To investigate the physical conditions in the ionized gas, we compare the observed line intensities with the photoionization model used by Ulrich & Péquignot (1980) in their study of the extended nebulosity in the Seyfert 1 galaxy NGC 3516. They used an optically thick model with approximately solar abundances and an input power law ionizing spectrum with index −1. They included empirical charge transfer rates which influence the low and intermediate ionization stages. The model produces line intensities, relative to Hβ, as a function of the ionization parameter ϕ/n_H where $\phi = L_\nu(4\pi R^2 h\nu)^{-1}$ photon cm^{-2} s^{-1} ryd^{-1} and n_H is the hydrogen density. For the extended emission with an ionizing flux appropriate to the mean radial distance from the nucleus of 8 kpc, a χ^2 test gives a best value for ϕ/n_H of 3.4×10^7 photon cm s^{-1} ryd^{-1} which corresponds to $n_\mathrm{H} = 2$ cm^{-3}. The total Hβ luminosity of this region then implies that the mass of ionized gas responsible for the extended emission is $\sim 10^8 M_\odot$. For the region closer to the nucleus, using the line intensities within the *IUE* aperture, the best fit is obtained for a slightly higher ionization parameter of 5.7×10^7 photon cm s^{-1} ryd^{-1}. This corresponds to a density of

$$n_\mathrm{H} = 72/R^2\,(\mathrm{kpc})\ \mathrm{cm}^{-3}.$$

Aside from the decreasing [O III]/[O II] ratio, the most convincing evidence that the ionization parameter decreases with increasing distance from the nucleus is provided by the dramatic fall in the [Ne V] $\lambda 3425/H\beta$ ratio away from the centre. This is to be contrasted with the relative constancy of the He II/Hβ ratio. A detailed discussion of the elemental abundances in the ionized gas is deferred to a later paper, but with a simple empirical analysis giving $12 + \log(O/H) \sim 8.4$, we are clearly not observing recently captured primordial gas.

3.2 GEOMETRY AND KINEMATICS

The distribution on the sky of the ionized gas can be studied from the photographs and from the high-dispersion, long-slit observations. Fig. 5 shows a sketch of the extent of the [O III] lines along the slit in the different position angles, which can be compared with the S-shaped structure seen in Plate 3. The condensation 7.5 arcsec to the west of the nucleus corresponds to the bright peak of emission seen in the [O III] lines at PA 90° (Plate 1) and indeed it is likely that line emission is responsible for all of the non-elliptical structure seen on the masked photograph. The faint, more extended structure seen on the high-contrast photograph (Plate 2a) may, however, be either line or continuum emission.

A remarkable feature of the [O III] line profiles away from the nucleus is their great breadth. To avoid the ambiguities which would therefore be present in a single-velocity contour map, we have in Fig. 6 illustrated the mean $\lambda 5007$ line profile at an array of points over the object. The broad wings, most clearly evident in the nuclear profile, can be seen extending away from the systemic velocity at large distances from the nucleus. This is particularly marked to the west and south-west where the line is over $350\,km\,s^{-1}$ broad (FWZI). Such behaviour is quite different from that seen in normal rotation curves where, due to integration along the line-of-sight in an inclined system, any wing would be expected on the side of the peak towards the systemic velocity.

Velocity curves corresponding to the line peaks for three slit position angles are shown in Fig. 7. These demonstrate the very sudden change in velocity across the nucleus which can be interpreted as a gradient of greater than $150\,km\,s^{-1}\,kpc^{-1}$. Some limited information about the stellar velocity field may be gained from the low-dispersion, long-slit observation at PA 90°. Fig. 8 shows two spectra around the Ca II *K*-line from regions 4 kpc on either side of the nucleus. No detectable velocity difference can be seen in the absorption lines,

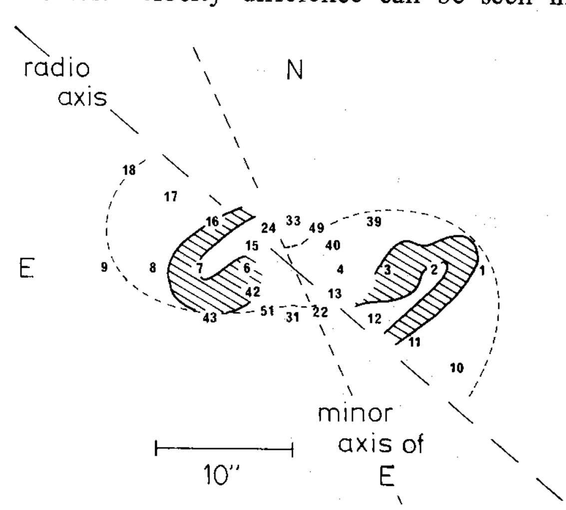

Figure 5. A sketch of the distribution of [O III] emission. The dashed lines represent the limits of emission deduced from the high-dispersion spectroscopy. The shaded area is the S-shaped structure seen on the masked photograph. The numbers correspond to the line profiles shown in Fig. 6.

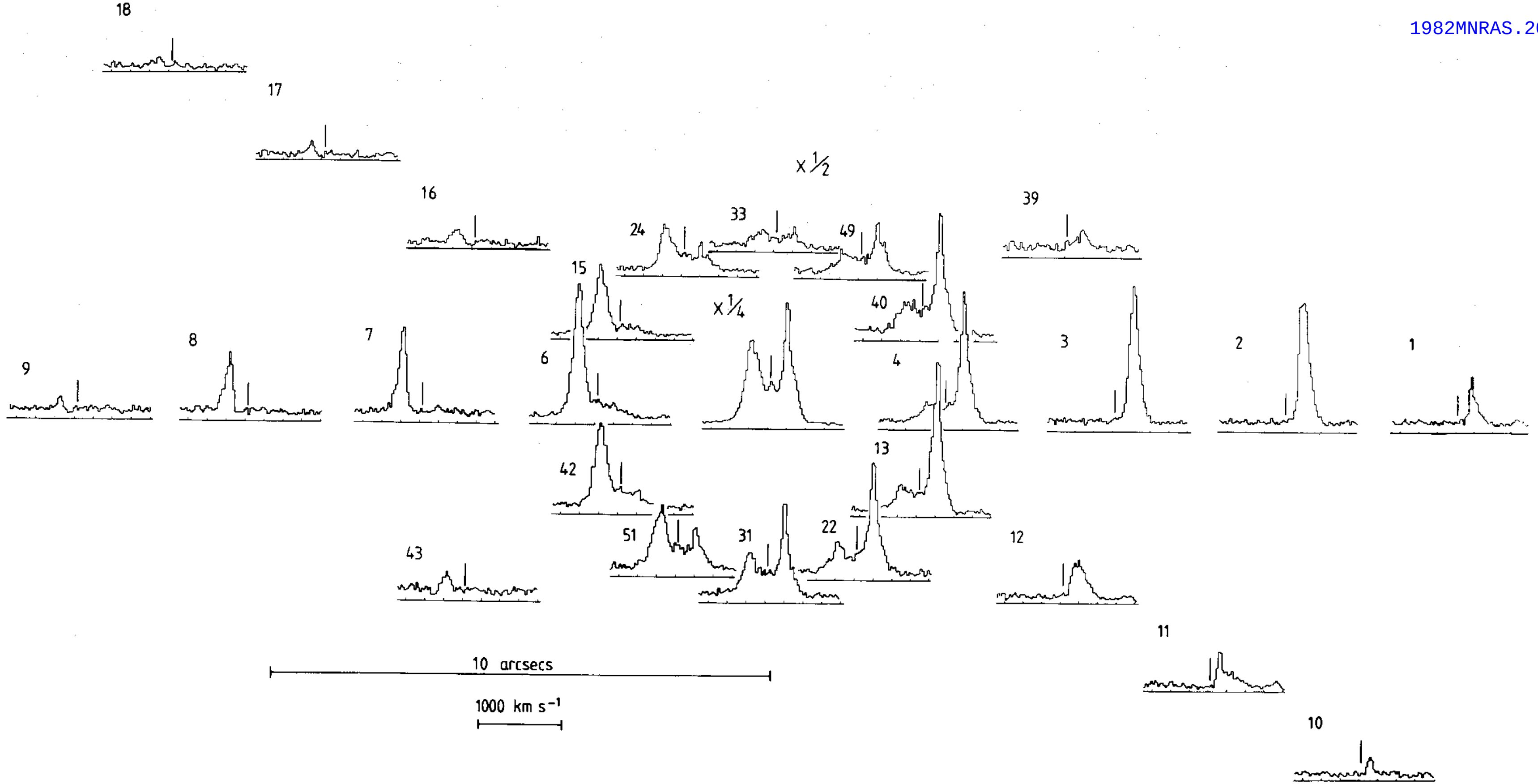

Figure 6. A map of the [O III] λ 5007 line profiles form the high-dispersion spectra. The profiles are sums of six spatial increments and the profile number is reproduced on the sketch in Fig. 5. Note that the intensity scale is reduced by a factor of 2 for the inner ring and a factor of 4 for the central profile.

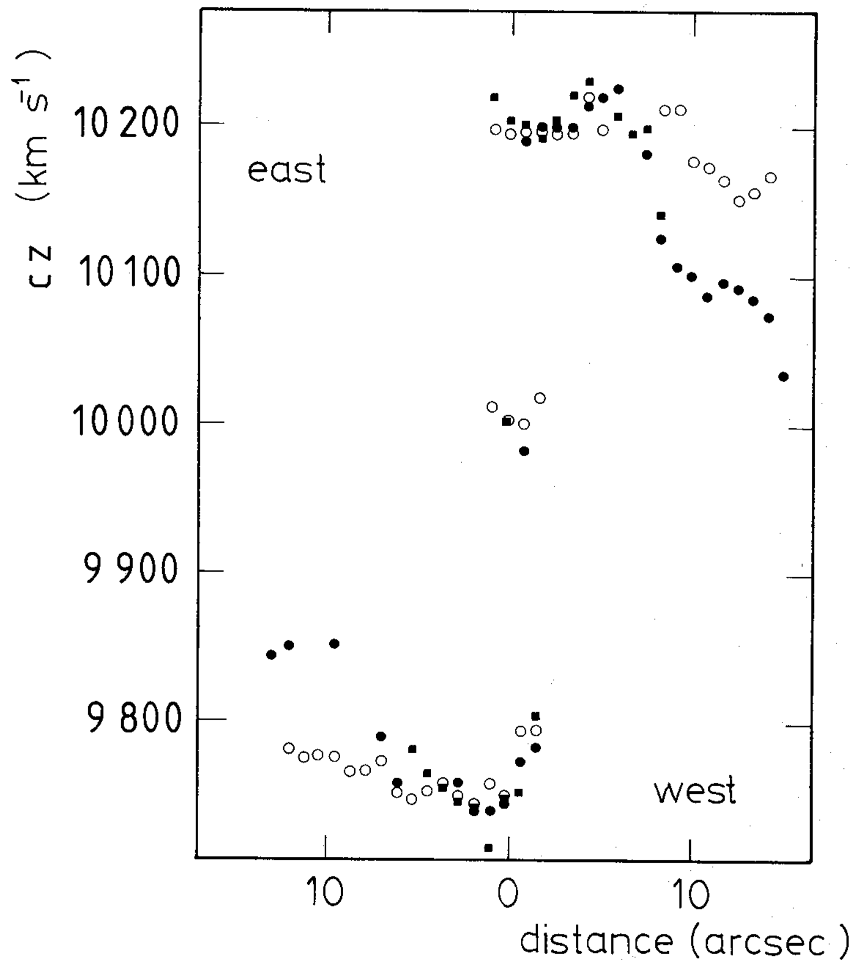

Figure 7. [O III] line peak velocities as a function of radial distance from the nucleus for three different positions angles ○ PA 90°, ● PA 60°, ■ PA 120°. Correct rest-frame velocity differences Δv_c are given by $\Delta v/1.033$.

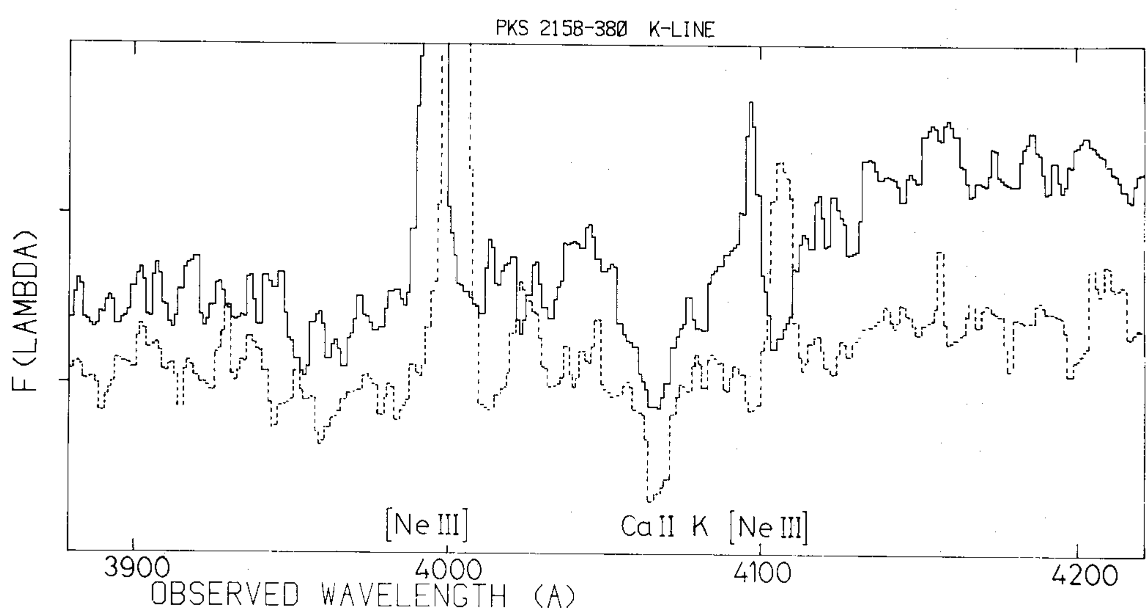

Figure 8. Low-dispersion IPCS spectra around the Ca II *K*-line from regions centred 4 arcsec either side of the nucleus to the east and west. This shows the different kinematic behaviour of the stars and gas.

amounting to a limit on the gradient of $< 10\,\mathrm{km\,s^{-1}\,kpc^{-1}}$. The mean absorption-line velocity, however, agrees with that of the emission lines to within the absorption-line error of $100\,\mathrm{km\,s^{-1}}$. Our observations contain no information about possible absorption-line gradients at other position angles.

4 Discussion

If the *IUE* observations do indeed indicate the presence of a nucleus emitting a power-law continuum, then we have shown that it is possible for this to ionize the gas throughout the entire galaxy. The comparison between the ionizing and the emission-line fluxes does nevertheless impose the constraint that the gas be distributed in such a way as to intercept most of the nuclear radiation and a substantial fraction of it at large radial distances. Our task now is to find a geometrical interpretation which is consistent with both the physical and kinematic state of the gas.

Aside from the presence of the ionized gas and the faint extended structure seen on the high-contrast photograph, PKS 2158 – 380 appears to be a normal E3 galaxy. The conclusion is consistent with the *UBV* and *JHK* photometry. The most notable feature of the radio structure is the flux asymmetry between the north-east and south-west lobes. The ratio of 5 is rarely found for radio galaxies of this luminosity (e.g. Ekers *et al.*, in preparation). Since the galaxy is not close to the apparent centre of the group, this may be a result of a gradient in the properties of the intergalactic medium rather than an asymmetry in the radio-source generating mechanism. The axis of the double source (PA $50° \pm 2°$) is neither parallel nor perpendicular to the axis of elongation of the emission-line region. The minor axis of the elliptical light distribution (PA $25° \pm 5°$) remains constant for different isophotal levels and also does not coincide with the radio axis.

The spatial distribution and velocity field of the ionized gas could be the result either of rotation in the gravitational field of the elliptical, or of some predominantly radial flow associated with the nuclear activity and the presence of extended radio structure. Whichever of these dynamical situations applies, we have already argued that the *ionization* of the gas is due to radiation from the active nucleus. The arguments which follow are an attempt to justify our conclusion that the observed velocity field is due primarily to rotation rather than radial motion and that, although the radio source and the extended optical emission are related phenomena, they are related by events at the nucleus rather than by any spatial coincidence on a larger scale. The long-slit emission-line spectra broadly suggest a simple rotating disc structure, but there are considerable differences of detail which provide clues to the actual dynamical state of the system.

The discussion of photoionization by the nucleus and the resulting requirement for a large sky coverage, together with the kinematic evidence and the form of the faint outer morphology, suggest that the interstellar medium in the elliptical galaxy has been influenced by, or has resulted from, a recent tidal encounter. Material accreted with finite angular momentum on to an elliptical galaxy will begin to settle into a disc. If the axis of angular momentum does not coincide with a symmetry axis of the dominant gravitating mass, the disc will be forced to precess and become progressively warped (e.g. Tubbs 1980). It may even be possible for a warp to exist in a reasonably steady state around a triaxial galaxy rotating about one of its principal axes (van Albada, Kotanyi & Schwarzschild 1982). The hypothesis of such a warped disc in the case of PKS 2158 – 380 is immediately successful in explaining a number of the observed properties.

The differential precession which results in a warped structure will allow radiation from the nucleus of the galaxy to travel large radial distances before intercepting the gaseous sheet and producing photoionization. This of course requires that the gas close to the nucleus settles into a disc-like configuration with only a small sky-coverage factor. Within the region of solid-body rotation this probably does happen, even if precession does occur, since its period will not depend on radius (e.g. Lynden-Bell 1965) and a disc would therefore precess as a coherent structure. In such a system, if the radio source axis is determined by the configuration of the interstellar gas very close to the active nucleus, there is no need for this direction to bear any relation to the apparent rotation axis deduced from observations made at much larger radii.

Viewed from most directions, the projection of a luminous, optically thin, warped disc on to a plane produces an S-shaped locus of maximum brightness. The same S-shaped locus will also have a complex radial velocity structure due to the line-of-sight coincidence of rings of different radius and inclination. This model therefore predicts that the extended emission of highest surface brightness will also tend to show the broadest lines. To help illustrate these points, Fig. 9 is a representation of a warp where each successive ring is given an equal increment in both position angle and inclination to the line-of-sight. Although this figure is only schematic, it is drawn with an orientation which does approximately represent the galaxy as illustrated in Figs 5 and 6. As Tubbs (1980) has attempted to do in the case of Centaurus A, the detailed dynamical modelling of such systems gives hope of allowing some deductions about the shape and mass distribution of the parent elliptical galaxy. The modelling of gas rather than stellar motions carries inherent difficulties, but emission-line systems like PKS 2158 – 380 allow velocity measurements to be made to far greater radial distances than is possible using absorption-line techniques. A full understanding of the gas motions must, however, await a much more complete spatial sampling of the two-dimensional velocity field than is provided here with a small number of slit spectra.

Although we have suggested a recent tidal encounter to explain the kinematic state of the gas, the photographs show no obvious close companion. It seems possible therefore that a small, gas-rich galaxy has been completely disrupted by its passage close to a massive elliptical: a merger as proposed by Toomre (1977). The configuration we observe now will not be in equilibrium. Both captured stars and gas will be subject to dissipational processes and will try to settle into a plane of symmetry, although the time-scales for the two will be different. This dissipational settling of the gas will result in a net inward flow of material which, in an elliptical galaxy, may be necessary for fuelling the active nucleus, a proposal

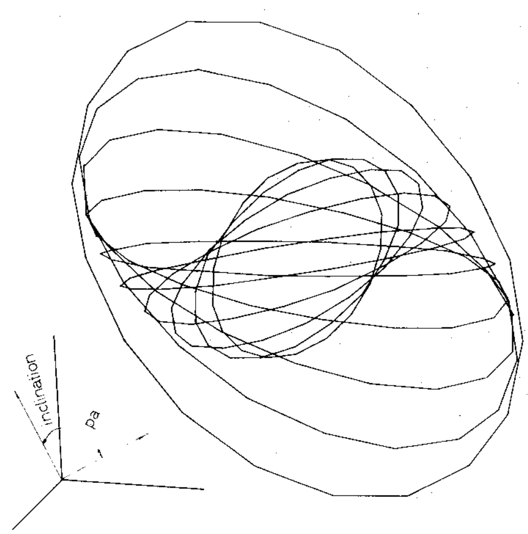

Figure 9. A sketch showing a warped disc schematically represented by a series of rings tilted with respect to one another by equal increments of 10° in position angle and inclination to the line-of-sight.

made earlier by Silk & Norman (1979). The fact that the elemental abundances in the ionized gas appear not to be abnormally low also argues in favour of the capture of an existing galaxy rather than primordial material from the integalactic environment.

5 Conclusions

We have shown that the extended emission lines in PKS 2158 – 380 could result from photoionization by a nuclear source of ultraviolet radiation. The particular geometrical constraint of large sky coverage imposed by such an hypothesis can be satisfied rather naturally by assuming the gas to be distributed in the form of a severely warped disc. The warp could be caused by differential precession following the capture and disruption by the elliptical of a small gas-rich companion galaxy, although a steady-state warp can exist around a rotating triaxial spheroid. The tendency of the gas to dissipate and settle into a plane of symetry provides a net of radial inflow of material to fuel the nuclear activity.

In PKS 2158 – 380, there is no spatial correspondence between the extended optical and radio emission regions. This phenomenon thus appears to be different from some other known cases of extended optical line-emission regions in radio galaxies (Miley *et al.* 1981) where there is a close relationship with radio jets and the gas is presumably ionized locally by the presence of a relativistic plasma. To make further studies of the origin and dynamical evolution of the ionized gas, detailed two-dimensional measurements of the velocity field in this and three other elliptical radio galaxies have been obtained using a scanning Fabry–Perot device (Taylor & Atherton 1980). These results will be published elsewhere.

Acknowledgments

We thank the ESO staff at La Silla and also John Fordham and Keith Shortridge for making it possible to use the IPCS on the 3.6-m telescope. The Director of the AAO and David Malin kindly made available the plate and provided the prints of PKS 2158 – 380. Ron Ekers, Peter Shaver and Alan Moorwood made data available to us in advance of publication. The FST is operated with the financial support of the Australian Research Grants Committee and the University of Sydney. We thank Arthur Watkinson for help with the Fleurs observations. RAEF was a guest observer at the VLA; the National Radio Astronomy Observatory is operated by Associated Universities, Inc. under contract with the US National Science Foundation. We also express our gratitude to the staff of the European Space Agency's Villafranca Satellite Tracking Station for their able support of the *IUE* observations. RAEF was an ESO fellow during part of this investigation.

References

Baldwin, J. A., Carswell, R. F., Wampler, E. J., Smith, H. E., Burbidge, E. M. & Boksenberg, A., 1980. *Astrophys. J.*, **236**, 388.

Bergeron, J., Maccacaro, T. & Perola, C. G., 1981. *Astr. Astrophys.*, **97**, 94.

Boksenberg, A., 1978. *Proc. of the ESO Conference, Optical Telescopes of the Future, December 12–15 Geneva*, p. 497.

Boksenberg, A., Snijders, M. A. J., Wilson, R., Benvenuti, P., Clavell, J., Macchetto, F., Penston, M., Boggess, A., Gull, T. R., Gondhalekhar, P., Lare, A. L., Turnrose, B., Wu, C. C., Burton, W. M., Smith, A., Bertola, F., Capaccioli, M., Elvis, A. M., Fosbury, R., Tarenghi, M., Ulrich, M.-H., Hackney, R. K., Jordan, C., Perola, C. G., Roeder, R. C. & Schmidt, M., 1978. *Nature*, **275**, 404.

Bolton, J. G., Clarke, M. E. & Ekers, R. D., 1965. *Aust. J. Phys.*, **18**, 627.

Bolton, J. G. & Shimmins, A. J., 1973. *Aust. J. Phys. astrophys. Suppl.*, No. 30.
Caldwell, N. & Phillips, M. M., 1981. *Astrophys. J.*, **244**, 447.
Christiansen, W. N., Frater, R. H., Watkinson, A., O'Sullivan, J. D., Lockhart, I. A. & Goss, W. M., 1977. *Mon. Not. R. astr. Soc.*, **181**, 183.
Clavell, J., Benvenuti, P., Cassatella, A., Heck, A., Penston, M. V., Selvelli, P. L., Beeckmans, F. & Macchetto, F., 1980. *Mon. Not. R. astr. Soc.*, **192**, 769.
Danziger, I. J., Goss, W. M. & Wellington, K. J., 1981. *Mon. Not. R. astr. Soc.*, **196**, 845.
de Vaucouleurs, G., de Vaucouleurs, A. & Corwin, H. G. J., 1976. *Second Reference Catalogue of Bright Galaxies*, University of Texas Press, Austin.
Fosbury, R. A. E., 1980. *ESO Messenger, No. 21*, p. 11.
Fosbury, R. A. E., Snijders, M. A. J., Boksenberg, A. & Penston, M. V., 1981. *Mon. Not. R. astr. Soc.*, **197**, 235.
Goss, W. M., Danziger, I. J., Fosbury, R. A. E. & Boksenberg, A., 1980. *Mon. Not. R. astr. Soc.*, **190**, 23P.
Graham, J. A., 1979. *Astrophys. J.*, **232**, 60.
Heckman, T. M. & Balick, B., 1981. *Astrophys. J.*, **247**, 32.
Holm, A., 1979. *SRC IUE Newsletter No. 4.*
Jenkins, C. R., 1981. *Mon. Not. R. astr. Soc.*, **196**, 987.
Jenkins, C. R. & Scheuer, P. A. G., 1980. *Mon. Not. R. astr. Soc.*, **192**, 595.
Kotanyi, C. G. & Ekers, R. D., 1979. *Astr. Astrophys.*, **73**, L1.
Krolik, J. H. & McKee, C. F., 1978. *Astrophys. J. Suppl. Ser.*, **37**, 459.
Lynden-Bell, D., 1965. *Mon. Not. R. astr. Soc.*, **129**, 299.
Miley, G. K., Heckman, T. M., Butcher, H. R. & van Breugel, W. J. M., 1981. *Astrophys. J.*, **247**, L5.
Mills, B. Y., Slee, O. B. & Hill, E. R., 1961. *Aust. J. Phys.*, **14**, 497.
Oke, J. B., 1974. *Astrophys. J. Suppl. Ser.*, **27**, 21.
Osterbrock, D. E., 1974. In *Astrophysics of Gaseous Nebulae*, p. 66, W. H. Freeman & Co., San Francisco.
Penston, M. V. & Fosbury, R. A. E., 1978. *Mon. Not. R. astr. Soc.*, **183**, 479.
Searle, L. & Bolton, J. G., 1968. *Astrophys. J.*, **154**, L101.
Seaton, M. J., 1978. *Mon. Not. R. astr. Soc.*, **185**, 5P.
Seaton, M. J., 1979. *Mon. Not. R. astr. Soc.*, **187**, 73P.
Silk, J. & Norman, C., 1979. *Astrophys. J.*, **234**, 86.
Simkin, S. M., 1979. *Astrophys. J.*, **234**, 56.
Snijders, M. A. J., 1980. *SRC IUE Newsletter No. 5.*
Taylor, K. & Atherton, P. D., 1980. *Mon. Not. R. astr. Soc.*, **191**, 675.
Toomre, A., 1977. In *Evolution of Galaxies and Stellar Populations*, eds Tinsley, B. M. & Larson, R. B., Yale University Observatory.
Tubbs, A. D., 1980. *Astrophys. J.*, **241**, 969.
Ulrich, M. H. & Péquignot, D., 1980. *Astrophys. J.*, **238**, 45.
van Albada, T. S., Kotanyi, C. G. & Schwarzschild, M., 1982. Preprint.